A mini scanning device for profiling charged beams

Patrick Moretto-Capelle, Eric Panader, Laurent Polizzi, Jean-Philippe Champeaux

A mini scanning device for profiling charged beams

P.Moretto-Capelle[a], E.Panader, L.Polizzi, J.P. Champeaux

Laboratoire Collisions Agrégats et Réactivité (LCAR), UMR5589 Université de Toulouse (UPS) and CNRS, 118 Route de Narbonne, F-31062 Toulouse, France

In this article we present the development of a mini scanner device to characterize the full transverse spatial density of a charged particle beam using computed tomography. The profiler consists of a wire mounted on a linear translator that can rotate around the beam. Tests were performed on a millimeter electron beam with 200 eV energy and 100 nA intensity, which allowed us to control and monitor both beam focusing and deflection.

I. INTRODUCTION

Beam diagnostic is of great importance nowadays for monitoring beam position, intensity and size. Position monitoring serves to correct beam position[1], control of the shape serves to optimization of the intensity in a given region for focalization purpose or looking for optimization of the of the irradiation area which is crucial in therapy applications such as proton or hadontherapy[2].

For this purpose, several control techniques have been proposed.

The assembly of microchannel plates coupled to a phosphor screen [3,4] [5,6] allows direct imaging of the beam profile and its position for electrons, ions and the neutral beam as well as UV and X-ray photons. Care must be taken to ensure a direct match between the input signal and the corresponding image and not to saturate the MCP by lowering the input flux with several grids each corresponding to 90% attenuation. This technique is destructive because the beam is no longer available afterwards. Scintillator detectors coupled to CCD camera can be also used [7]. Interaction of high energy beams with residual gas will created secondary particles which will be detected by MCP and imaged by CCD device [8].

Quasi non-destructive techniques using wires are also used such as harps or moving wires and the combination of two perpendicular assemblies gives profiles in the corresponding directions [9].

Such a principle has been developed for H^- beams using the photo-detachment process with a laser wire[10], in this case no real wire is used to avoid heating and destruction in the case of high intensity and high energy ion beams.

However the problem of measuring profiles in two orthogonal directions does not allow a complete determination of the beam profile but still gives the beam position. For inhomogeneous and/or aspherical beams, this method is no longer sufficient and more sophisticated techniques are required. Multiplying the measurements of one-dimensional profiles over several angles leads to the computed tomographic (CT) principle well known in medical applications and thus allows the full two-dimensional density to be reconstructed numerically.

CT has already been used in beam diagnostic to measure the phase space distribution: McKee et al.[11] have proposed a new technique that combines CT and quadrupole scanning to reconstruct, without any assumptions, the transverse phase space distribution (and thus calculate the emittance) for a MeV electron beam.

Nanometer beam profiling using CT has been applied to an electron beam a few 10 nanometers wide, and the detection wire is a single-walled nanotube 0.4 nm in diameter[12]. On the other hand, for high-current, large, proton beams, which are often irregularly distributed[13], CT must be used. For this, Xing et al[13] has designed a rotating multi-wire scanner with 19 carbon wires spaced 3 mm apart and a sophisticated complementary translation mechanism enabling 0.1 mm linear scanning.

In this paper, we present a scanner device that is simple, easy to build, and inexpensive, using only a single wire for the profiling of a charged particle beam.

II. TOMOGRAPHY PRINCIPLE: THE RADON AND INVERSE RADON TRANSFORM

Tomography is a widely used technique in medical imaging (see 13 and references therein). It is based on the measurement of the attenuation of X-rays by the material they are passing through.
The Berr-Lambert law, which describes this attenuation, is given by the equation:

$$I(\Lambda) = I_0 e^{-g(\Lambda)} \quad (1)$$

Where $g(\Lambda)$ is the integral of the attenuation function $\mu_z(x,y,z)$ along Λ path, corresponding to the straight line followed by the X-rays through the material between the X-ray source and the detector :

$$g(\Lambda) = \int_{\Lambda} \mu(x,y,z).dl \quad (2)$$

In the following we will work at a given z and the paths Λ_i are in the x,y plane as describe in figure 1

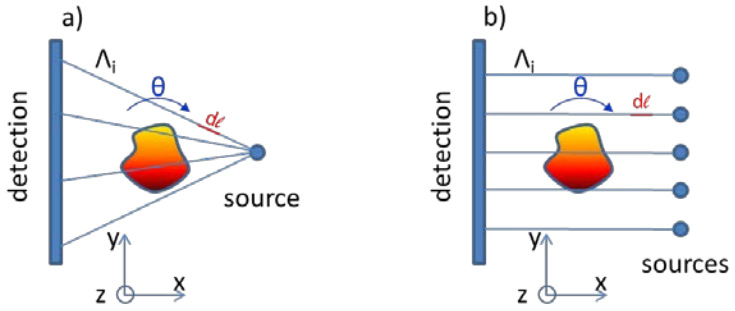

Figure 1: Principle of RX tomography a) with a ponctual x ray source, b) parallel beams

By rotating the source relative to the object and recording the intensities on appropriate detectors (see figure 1), it is possible to obtain a complete set of g(Λ) values whose inverse Radon transformation gives the attenuation function profile μ(x,y,z) at given z. By repeating the operation for different z, we can then produce the 3D density profiles of the traversed materials.

A. Case of charged particles beam profiling: What do we measure?

We propose to use this technique for charged particles beam density profile.
Let $\vec{J}$ the courant density, the intensity dI of the beam current is given by $dI = \vec{J}.\overrightarrow{dS} \sim J.dS$ for quasi parallel beam and a surface perpendicular to the beam velocity supposed to be along the z direction.
J(x,y,z) is the density of current we want to determine at a given z (noted hereafter $J_z(x,y)$) and corresponds to the beam profile. In order to obtain $J_z(x,y)$, we will scan the beam in the (x,y) plan using a thin wire (in red in figure 2) perpendicular to the scanning direction (in blue) whose length is larger than the beam section and measure integrated current produce by the beam on it. The scanning procedure is comparable to the one showed in figure 1-b.

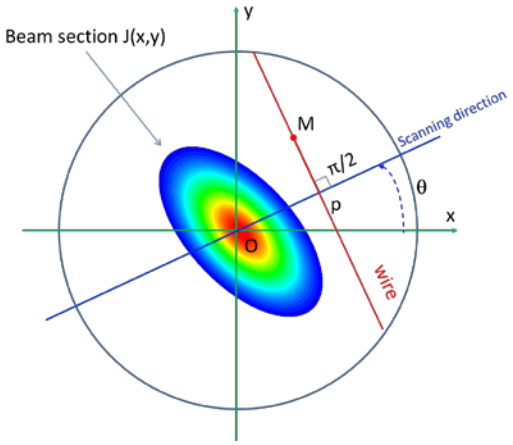

Figure 2: Geometry of the scanning apparatus

Here the detector is the wire itself whose position is defined by two coordinates namely the distance OP = p (the wire is perpendicular to OP) and the angle θ between the scanning direction and the x axis. The intensity is defined as:

$$g_\theta(p) = \iint_{wire} J_z(x,y).dl \tag{3}$$

A point M(x,y) on the wire, assumed to be infinitely thin, obeys the equations:

$$\begin{aligned} &\overrightarrow{OM} = \overrightarrow{OP} + \overrightarrow{PM} \\ &\overrightarrow{OP}.\overrightarrow{OM} = \overrightarrow{OP}.\overrightarrow{OP} \\ &x.cos\theta + y.sin\theta = p \end{aligned} \tag{4}$$

Then we can rewrite integration (3) in order to run over all the surface by introducing $\delta(x.cos\theta + y.sin\theta - p)$ where x,y is a coordinate of a point M on the surface :

$$g_\theta(p) = \iint J_z(x,y).\delta(x.cos\theta + y.sin\theta - p).dx.dy \tag{5}$$

which define the Radon Transform[14]. Note that $g_\theta(p)$ is completely equivalent to the $g(\Lambda)$ expression

B. Reconstruction of the density of current distribution $J_z(x,y)$

In a general way, let us define the two-dimensional Fourier transform:

$$J_z(x,y) = \iint F(u,v).\ e^{2i\pi(u.x+v.y)}dudv \tag{6}$$

Taking the Fourier Transform of g_θ on the variable p, we have :

$$G_\theta(\omega) = \iint dx.dy.J_z(x,y) \int dp.e^{-2i\pi\omega p}.\delta(x.cos\vartheta + y.sin\theta - p) \tag{7}$$

And so:

$G_\theta(\omega) = F(\omega.cos\theta, \omega.sin\theta)$

through the change of the variable (polar coordinates) u= $\omega.cos\theta$, v= $\omega.sin\theta$, du.dv=$|\omega|.d\omega.d\theta$

$$\begin{aligned} J_z(x,y) &= \iint F(\omega.cos\theta, \omega.sin\theta).e^{2i\pi.\omega.(cos\theta.x+sin\theta.y)}.|\omega|.d\omega.d\theta \\ J_z(x,y) &= \int d\theta \int d\omega.|\omega|.G_\theta(\omega,\theta).e^{2i\pi.\omega.(x.cos\theta+y.sin\theta)} \\ J_z(x,y) &= \int d\theta.\boldsymbol{TF^{-1}}[|\omega|.G_\theta(\omega,\theta)]\ (x.cos\theta + y.sin\theta) \end{aligned} \tag{8}$$

If we assume a discrete measurement at equidistant angles, we get:

$$J_z(x,y) \sim \Delta\theta.\sum_{\theta_k} \boldsymbol{TF^{-1}}\ [|\omega|.G_{\theta_k}(\omega)](x.cos\theta_k + y.sin\theta_k) \tag{9}$$

This defines the inverse Radon transform by filtered backprojection[15]. Then from measuring current intensity on the wire for each p position and each θ orientation around the beam we can go back to beam density profile $J_z(x,y)$.

III. EXPERIMENTAL SET-UP

A. Mechanical assembly

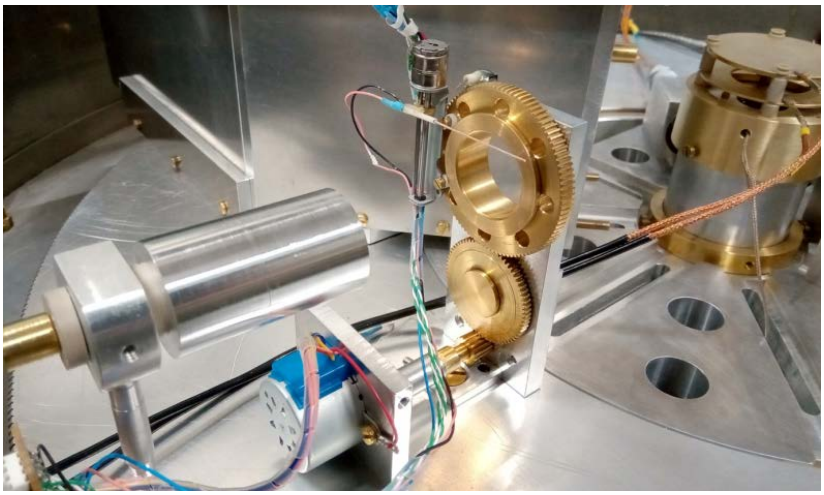

Figure 3: Installation of the scanner device inside the collision chamber, on the left, the Faraday cup used to measure the beam intensity

The mechanical assembly is shown in figure 3. The assembly is made of brass and aluminum (AU4G) in order to minimize the magnetic stray fields which can be of importance for low energy electron beam density profile measurement for example, Ferrite shields can also be used to shield motors. The wire used is made of copper, has a diameter of 0.4 mm and is sufficiently stiff. This is important because, unlike other scanning devices[12,13], the wire is only attached at one end.

The working surface of the developed scanner is a 25 mm diameter disk, the diameter of the scanned beam should therefore not exceed 25mm. A three-part brass gear (purchased from HPC (https://shop.hpceurope.com/fr), each with a pitch diameter of 9mm, 35mm, 50mm) rotates the linear scanning part. Only 0.5 module (ratio of the pich circle diameter to the number of teeth, gears will only mesh with each other if they have the same module) gears are available. The largest gear has been modified to fit our assembly in order to create an empty disc with a diameter of 25mm to allow the beam to pass through the scanner. The gearwheels are attached to the Dural support by brass parts. These have been carefully adjusted to ensure good mechanical centering, but also to minimize friction. A 0.02 mm mechanical tolerance was a good compromise. A number of motors were tested (to find the one with the right characteristics in size and torque) and a different support was made for each of them.

B. Electronic control

In order to measure $g_{\theta_k}(p)$ (see eq. 5), we have to carry out a controlled 180° rotation (with a good angular precision) and, at each angle, a linear scan (see figure 2) with a measurement of the current on the wire. To do this, we use two low cost commercial 5V stepper motors, namely:

i)_a 28BYJ-48 for rotation with a high resolution of 2048 steps per revolution which coupled with the gear reduction (5.555) gives a resolution of 0.0315 degree/step on the rotating part.

ii)_a DFRobot FIT0708 assembly for the wire translation is consisting of a 20 steps per revolution stepper motor coupled to a threaded rod and a linear displacement screw. This results in a resolution of 20 μm/step in the translational part.

The rotation and scanning sequences are programmed on an Arduino Uno microcontroller and the Adafruit Motor/Stepper/Servo Shield for Arduino v2 Kit - v2.3 allows us to simply drive the rotation of the two motors by an adapted library (figure 4).

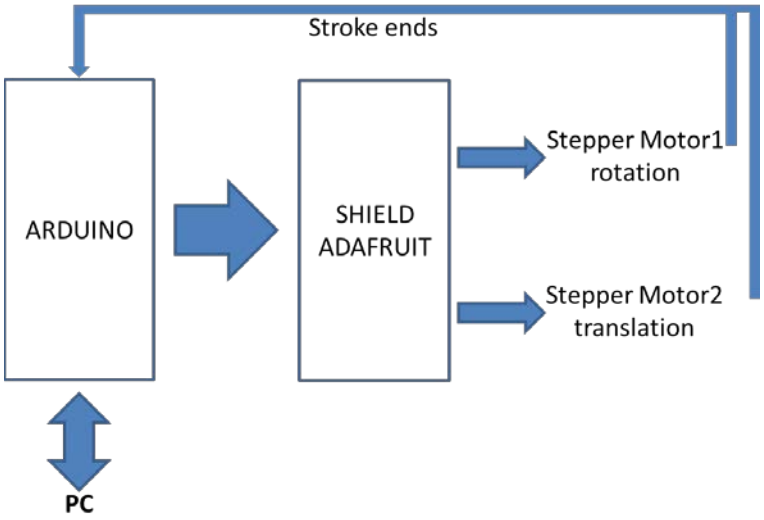

Figure 4 :Synoptic scheme of the motor driving

With the homemade stroke ends, the initial rotation angle positioning as well as the initial scan position are realized and verified during the scanning process.

The total beam intensities that we use in our research applications range from ~100nA to ~µA. and the current measured on the wire is about ~1-10nA . A conversion current voltage is first processed through a resistor R=5MΩ and a capacitor CF=1nF is used for noise filtering. The corresponding voltage is then followed by an adjustable gain of 2-20-200 and the final tension corresponds to V=0.01-0.1-1*I(nA). Of course, the values may be subject to change for specific purposes.
The TLE2074ACN quadruple operational amplifier was selected for its FET (field effect transistor) inputs, which are designed for low input currents.
The voltage is inverted or not depending on the sign of the current measured on the wire, because the analog inputs of the Arduino must be positive and less than or equal to 5V. Finally, an offset compensation is applied because the TLE2074ACN quadruple operational amplifier does not have one. The electronic scheme is given in figure 5.

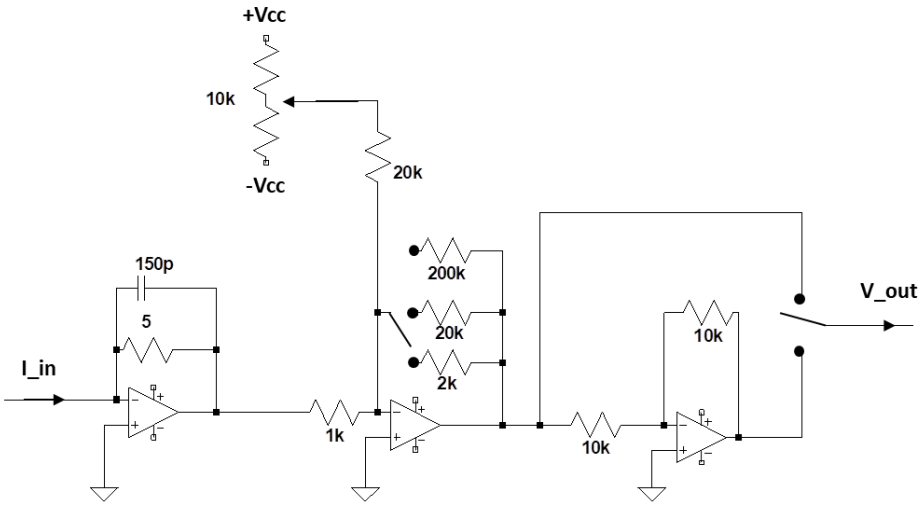

Figure 5: Electronic scheme of the current amplifier

The whole electronic assembly is illustrated in figure 6.
A special vacuum flange has been designed for the transmission of motor commands, limit switches and the wire signal between the external electronics module and the in-vacuum scanner.

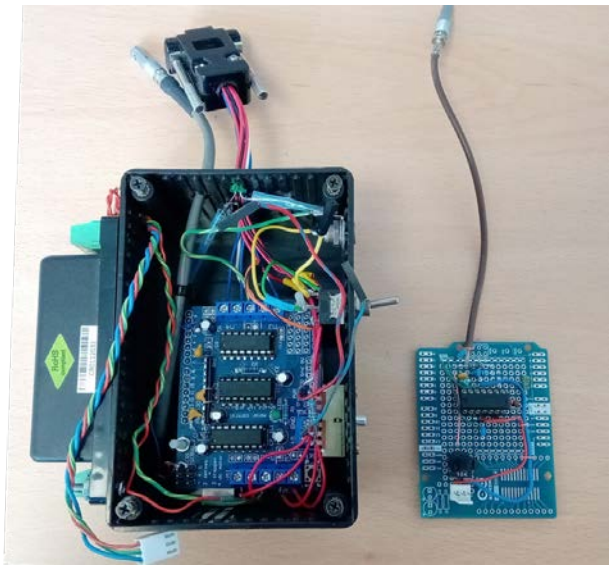

Figure 6: Electronic circuits. left: Arduino and Motor shield, right: home-made current amplifier shield

C. Computer monitoring

The selection of the angle step is done by means of a home-made code and send to the Arduino micro controller which begin the scan procedure in both angle and linear: the total area (25mm) must be done in 2^n steps adapted to the Fast Fourier Transform and 256 steps (0.1mm/step) are sufficient for beams with a diameter of a few mm. The data (position, angle and wire current) are sent from the Arduino board to the computer directly via the serial link (wireless transmission can also be used), are stored in a file and are plotted (sinogram) in real time. Finally, a C++ procedure using the direct and inverse Fast Fourier transforms is called to compute the inverse Radon transform implementing the eq. 9. Beam profile is plotted on screen and also stored into file.
A 256 point linear scan takes 3 seconds, the entire acquisition for a 10° rotation step from 0° to 170° takes 54 seconds, the inverse Radon transform calculation time is 2 seconds, so the entire procedure takes just a minute. Each scan on p is normalized so that the integral is equal to the beam current that was previously measured via a Faraday cup, the normalization avoids any fluctuation in the intensity of the beam, which can be a source of uncertainty in the inverse Radon transform.

D. Region of application and limits

Our mini scanner allows beams size of <25mm to be analysed. There is no limit for small width beam, nevertheless the wire diameter has to smaller than to the beam width in order to neglect it (the measured profile is a convolution between the wire diameter and the real beam profile). For wires with a diameter of a few tenths of a millimeter, the minimum beam size must be a few millimeters. Vibration of the wire due to translational motion must be minimized by reducing the corresponding translational speed.
Only continuous beams can be analysed and total intensity must be larger than 1nA.
Due to stepper motors, our device is not designed for ultra high vacuum.

IV.TESTS: EXPERIMENTAL RESULTS

The setup was set up in our collision chamber, in front of our electron gun, at a distance of about 20 cm. The electron gun was chosen for the tests because it is easier to change the focus and deflection.
Of course, the motors are not designed for vacuum. However, after two days of pumping, a residual pressure of 2.10^{-7} Torr can be achieved (the volume of the vacuum chamber is ~1.5 10^5cm3 and pumping is carried out using a 1000 l/s turbo pump). The first few runs of the scanner will cause quite a bit of degassing. This is due to the heating of the coils and the rotation of the motors.
For the tests, a 200eV beam was produced and a 10° step for the rotation was chosen.

A. Focalization of the beam

We have made images of the beam for two values of focus of the electron gun. The respective sinograms are given in figure 7. They are relatively flat indicating that the electron beam is rather centered. Moreover, the width of the curve is smaller in the

case than in the case revealing a smaller beam width. The 2D profile of the beam is obtained by applying the inverse Radon transform showing the full 2D profile of the beam.
The images confirm the previous deduction: the beam is quite centered (xc=-0.35± 0.04mm and yc=-1.3± 0.04mm) and the FWHM increases from 1.5± .2mm to 2.5± .2mm when the focalization is varied.

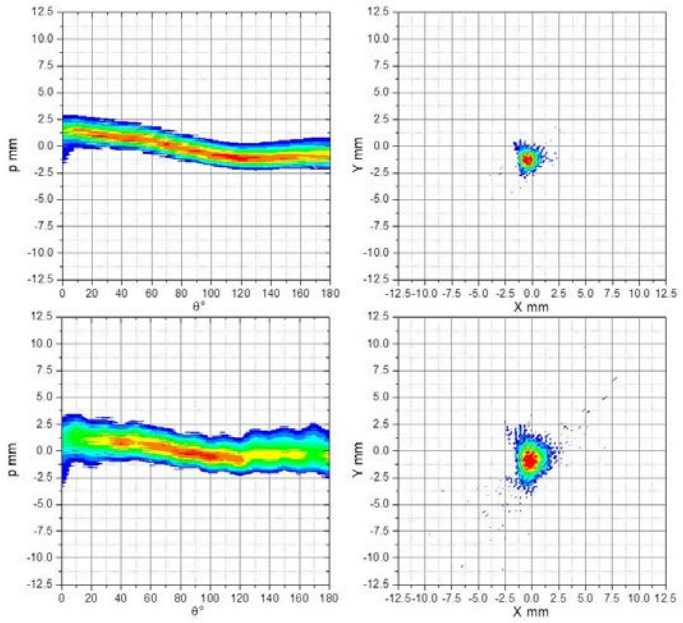

Figure 7: Effect of focalization. Left: sinogram, right: density. Top: good focalization, bottom: bad focalization

A control of the size of the beam is easily realized.

B. Deflection of the beam

We also checked the control of the position of the through the deflection. The focus of the electron gun is set at 300V. The sinograms, reconstruction and deflection electrodes and their polarization (verified in situ) are shown in figure 8.

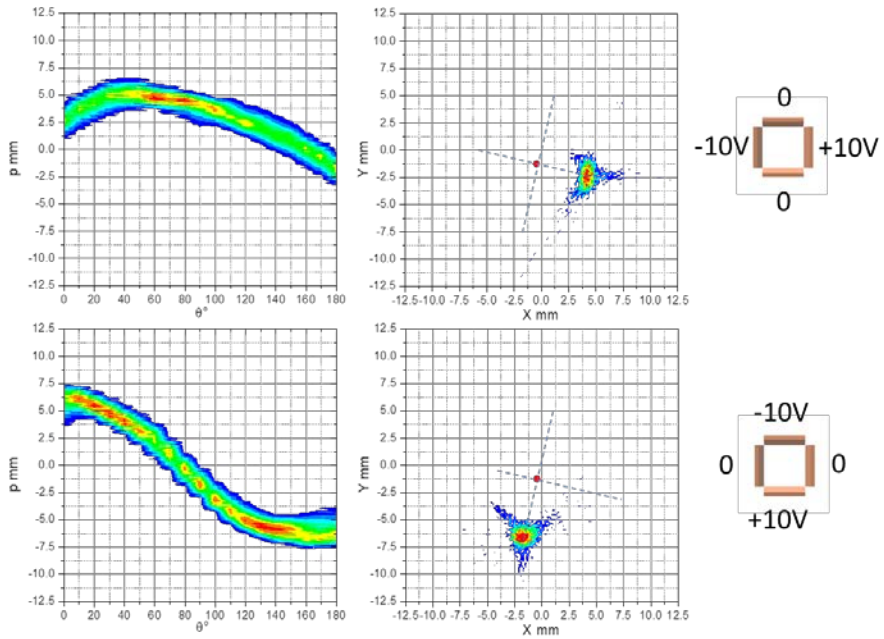

Figure 8: Effect of the deflection. Top: horizontal. Bottom: vertical

The beam is moved in the correct direction based on the polarization of the electrodes. The deflections are not strictly horizontal or vertical and both have undergone a 12° shift which is not due to the scanner imaging but to the rotation of the deflection electrodes in our electron gun positioning as shown in figure 9.

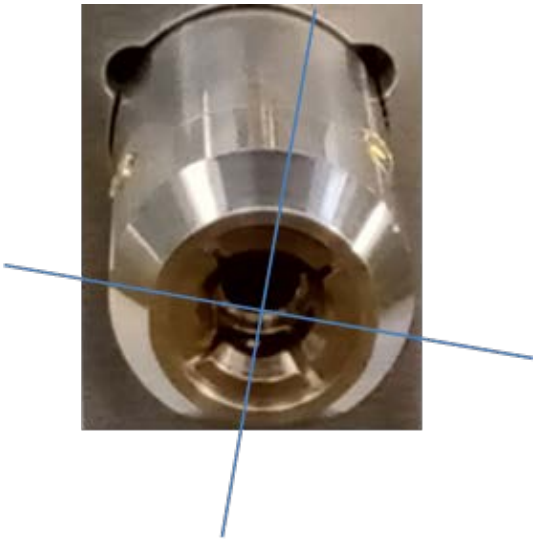

Figure 9: Rotation of the electron gun

The deflection of the beam (and corresponding displacement) is completely described by the scanner device and positioning defect of the electron gun has been revealed.

VI. CONCLUSION AND OUTLOOK

In this paper, we show the realization of a small charged diagnostic beam that allows the complete determination of the 2D current density at a given transverse position. For this purpose, we used the CT technique in which the beam is scanned at different angles. The technical implementation includes stepper motors for linear motion as well as high resolution rotation, mounted on precisely adjusted gears. An Arduino microcontroller is used to drive the stepper motors and acquire the current on the wire at each angle and position. The reconstruction of the density from all the measured profiles is done by inverse Radon transformation. The whole easy to use setup and the associated code/interface have been tested in the case of focusing and beam deflection and the expected behaviors have been found. One improvement to the setup is to reduce the wire diameter to ~0.2mm to increase resolution. Another mode of operation where the wire (grounded) does not measure the current but acts as a mask in front of a Faraday cage can be considered, the difficulty lies in measuring a small variation of current. A complete determination of the beam geometry and 3D current density can be obtained by moving the setup along the beam direction and creating profiles for different z-directions and interpolating between them.

REFERENCES:

[1] M. Gasior, R. Jones, T. Lefevre, H. Schmickler, and K. Wittenburg, in *Proc. CAS-CERN Accel. Sch. Adv. Accel. Phys.* (2013).

[2] F. Reaz, K.N. Sjobak, E. Malinen, N.F.J. Edin, and E. Adli, "Sharp dose profiles for high precision proton therapy using strongly focused proton beams," Sci. Rep. **12**(1), 18919 (2022).

[3] A. Khoukaz, D. Bonaventura, S. Grieser, A.K. Hergemöller, E. Köhler, and A. Täschner, "Two-dimensional visualization of cluster beams by microchannel plates," Nucl. Instrum. Methods Phys. Res. Sect. Accel. Spectrometers Detect. Assoc. Equip. **735**, (2014).

[4] J. Pitters, M. Breitenfeldt, S.D. Pinto, H. Pahl, A. Pikin, A. Shornikov, and F. Wenander, "Pepperpot emittance measurements of ion beams from an electron beam ion source," Nucl. Instrum. Methods Phys. Res. Sect. Accel. Spectrometers Detect. Assoc. Equip. **922**, (2019).

[5] I. YAMADA, N. OGIWARA, Y. HIKICHI, J. KAMIYA, and M. KINSHO, "Development of a Gas Distribution Measuring System for 2-D Beam Profile Monitor," Vac. Surf. Sci. **62**(7), (2019).

[6] A. Rohrbacher, and R.E. Continetti, “Multiple-ion-beam time-of-flight mass spectrometer,” Rev. Sci. Instrum. **72**(8), (2001).
[7] M. Rydygier, G. Mierzwińska, A. Czaderna, J. Swakoń, and M.P.R. Waligórski, “Studies of scintillator response to 60 MeV protons in a proton beam imaging system,” Nukleonika **60**(3), (2015).
[8] T. Tsang, S. Bellavia, R. Connolly, D. Gassner, Y. Makdisi, T. Russo, P. Thieberger, D. Trbojevic, and A. Zelenski, in *Rev. Sci. Instrum.* (2008).
[9] M. Dombsky, D. Bishop, P. Bricault, D. Dale, A. Hurst, K. Jayamanna, R. Keitel, M. Olivo, P. Schmor, and G. Stanford, “Commissioning and initial operation of a radioactive beam ion source at ISAC,” Rev. Sci. Instrum. **71**(2 II), (2000).
[10] Y. Liu, A. Aleksandrov, D. Brown, R. Dickson, C. Huang, C. Long, and C. Peters, in *IPAC 2013 Proc. 4th Int. Part. Accel. Conf.* (2013).
[11] C.B. McKee, P.G. O’Shea, and J.M.J. Madey, “Phase space tomography of relativistic electron beams,” Nucl. Inst Methods Phys. Res. A **358**(1–3), (1995).
[12] M.D. Zotta, S. Jois, P. Dhakras, M. Rodriguez, and J.U. Lee, “Direct Measurement of the Electron Beam Spatial Intensity Profile via Carbon Nanotube Tomography,” Nano Lett. **19**(7), (2019).
[13] Q.Z. Xing, L. Du, X.L. Guan, C.X. Tang, M.W. Wang, X.W. Wang, and S.X. Zheng, “Transverse profile tomography of a high current proton beam with a multi-wire scanner,” Phys. Rev. Accel. Beams **21**(7), (2018).
[14] J. Beatty, “The Radon Transform and the Mathematics of Medical Imaging,” Colby Coll. **Honors The**, (2012).
[15] J.G. Marichal-Hernández, R. Oliva-García, Ó. Gómez-Cárdenes, I. Rodríguez-Méndez, and J.M. Rodríguez-Ramos, “Inverse multiscale discrete radon transform by filtered backprojection,” Appl. Sci. Switz. **11**(1), (2021).